

# Laminar Mixed Convection in Anannular Horizontal Elliptical Duct

*In this work, laminar mixed convection heating along a horizontal duct, formed by two concentric elliptical tubes under uniform and equal heat fluxes, is studied numerically using the finite volume method. The work focuses on the geometric effect of the duct passage section, where nine cases have been proposed, starting with the two cylinders case, followed by the case interior cylinder/exterior ellipse, then the opposite and finally the case with two ellipses.  $Re=100$  is taken for  $Pr=100$ . While a  $Gr$  ranging from  $0.0$  to  $5.0 \times 10^{+5}$  is supposed. The results for the base case for a circular cross-sectional area -encountered in the food processing industry- show after some distance from the entrance the formation of thermal stratification between the top and bottom of a section where the hotter fluid risks being denatured, with a strong slowdown in the flow at the top, which degrades the convective heat transfer and favors conductive one, particularly at high  $Gr$ . The other cases tested show that the case with two ellipses offers the best thermal homogeneity and considerably reduces the problem of the flow slowdown. This result is proposed as a solution for the thermal stratification problem.*

**Keywords:** Mixed convection, annular duct, Grashof number, thermal stratification, elliptic geometry.

## A. Horimek

Professor  
Mechanical Engineering Department  
Ziane Achour University  
Djelfa  
Algeria

## N. Ait-Messaoudene

Professor  
Mechanical Engineering Department  
University of Hail  
KSA

## 1. INTRODUCTION

In order to be sanitary in addition to being consumable for a long period, food products (fruit juices, dairy products, yogurt, etc.) are heated and then sterilized. The heating phase serves to kill the bacteria, while the sterilization phase prevents its reproduction. Each product has a suitable temperature for sterilization depending on its physical characteristics. The heating phase is carried out in annular heat exchangers with horizontal cylindrical pipes. This work proposes a geometric solution to remedy a problem encountered in this type of food industry which hinders the proper heating of the fluid to be sterilized. These fluids are characterized by a very high Prandtl number ( $Pr=O(100)$ ), which gives enormous lengths to reach full thermal development ( $L_{th}=O(Re \times Pr \times D_h)$ ). Generally the circulation of fluids is slow; a Reynolds number ( $Re$ ) close to 100 is generally used. In addition, the outer diameter ( $D_e$ ) is close to  $0.1m$  with an aspect ratio equal to 0.5. With these details, pipes with lengths of up to  $500m$  are used. For this, and in order to keep the heat exchanger of a reasonable size, a system of rows of horizontal pipes of length  $2.0$  to  $3.0m$  connected by elbows is used. That is, 10 to 20 horizontal pipes arranged in a serpentine shape upwards. Heating is ensured by uniform heat fluxes on the outer and inner cylinders of the same amounts and varying from  $1000W/m^2$  to  $8000W/m^2$  depending on the desired heating level, which changes depending on the fluid to be heated or the degree of sterilization to be ensured [1].

As  $Pr$  is significantly greater than 1.0, dynamic regime can be assumed established at the inlet [2]. Only thermal development matters. Due to ignorance at first, heat transfer along the pipe was assumed under forced convection. But, an unexpected thermal stratification was recorded after a certain distance from the entrance. This stratification is characterized by an accumulation of hot fluid at the top and less hot fluid at the bottom of a same section. The difference between high temperature and low temperature sometimes reaches  $25^\circ C$ . Consequently, the fluid at the top risks being denatured, in addition to being at a higher temperature than that suitable for sterilization. The error committed boils down to the neglect of the fluid density thermodependency. Heat transfer is under mixed convection in reality. The presence of natural convection causes the hot fluid to rise upwards and by continuity in the section, the less hot fluid moves downwards. Gradually, thermal stratification results. Extensive details of these observations can be found in [1], where numerical, experimental and asymptotic analyzes by linear stability analysis were carried out. The objective of the cited reference was to determine the position from which natural convection disrupts the flow. One speaks of the critical Cameron number ( $Z^*=2z/D_h \cdot Pe$ ). Many results were provided, pointing out that the length of the assumed pipe remains small compared to that ensuring the thermal development. The work was taken over in [3], where the numerical calculations were carried out up to the full thermal development. In the first part with concentric cylinders, the effects of the Grashof number ( $Gr$ ), the aspect ratio ( $D_i/D_o$ ), the pseudoplastic rheological index ( $n$ ), complete heating (two walls) or partial heating (one wall heated and the other isolated), in addition to the temperature-dependent effect on viscosity ( $\mu(T)$ ) have been extensively studied. Sub-

Received: July 2025, Accepted: March 2026

Correspondence to: Dr Abderrahmane Horimek  
Mechanical Engineering Department,  
Ziane Achour university of Djelfa, Algeria  
E-mail: a.horimek@univ-djelfa.dz

doi: 10.5937/fme2602269H

© Faculty of Mechanical Engineering, Belgrade. All rights reserved

FME Transactions (2026) 54, 269-280 269

sequently, an eccentricity in the annulus was proposed as a solution to reduce the degree of thermal stratification. It has been found that shifting the inner cylinder downward helps to widen the space between the cylinders at the top and thus reduces the accumulation of hot fluid following mixing with thicker layers on its upward path. The second supposed upward shift shows an amplification of thermal stratification by bringing the two cylinders together at the top, despite the reduction in the intensity of natural convection compared to the base case (concentric cylinders). Additional details have been reported in [4-5]. It should be noted that the proposal of applying an eccentricity between the cylinders showed a good reduction in thermal stratification, but the degree of eccentricity to apply depends on the physical properties and the heating conditions. This implies that the eccentricity must be changed from time to time when the fluid to be heated is changed or the heating conditions are changed. Without doubt, this creates a limitation of the solution from an industrial point of view. The second annoying point is that if the appropriate eccentricity is chosen, at elbows, the inner tube will have to slope downwards so that it remains positioned at the bottom in relation to the outer tube. With a number of elbows between 10 and 20, this will affect the process quite a bit. The third point lies in the strong reduction of velocity in the narrow zone, particularly at high eccentricity. This strong reduction gives rise to a tendency towards conductive rather than convective heat transfer. Although this third effect remains far from being encountered according to the results provided in [3;5], it should not be neglected.

From the above comes the thought of another solution that is simpler to integrate industrially and allows avoiding the disadvantages mentioned. As the cause of stratification is the initiation and intensification of natural convection, a work in this direction was carried out in [6] treating natural convection in an elliptical annular space. Fifty-four (54) geometries were assumed in order to clearly see the influence of the geometric shape on the distribution of the temperature field in the section. Results on the intensity of heating (average Nusselt), classified in descending order were also provided. From the work, it was found that the horizontal orientation of the ellipses (in the broad sense) offers more thermal homogeneity and heat transfer intensity. For this, only the horizontal orientation of ellipses is assumed in the present work, in which nine (09) geometries have been assumed, starting with the classic case formed by two cylinders (a cylinder is an ellipse with equal diameters), then an interior ellipse for an exterior cylinder, then the reverse, and finally two ellipses. Different lengths of the small diameter ( $D_{el-s}$ ) and the big diameter ( $D_{el-b}$ ) of the ellipse were tested. For all assumed cases, the two tubes are concentric, which is a practical advantage.

In this work, no interest is given to the intensity of heat transfer ( $Nu$ ). It can be summarized that its evolution, for the case of forced convection, shows a progressive decrease until stability which describes the full thermal development. Its maximum is at the inlet, where the fluid is still cold, therefore maximum heat flux enters from the walls. Gradually, the fluid

temperature increases and the amount of incoming flux decreases. After a certain distance, the heating reaches the middle of the annular space and the incoming amount stabilizes at its minimum value. The work in [7] offers various results on this subject in addition to very useful correlations for determining its values in several situations, in addition to the thermal development length, necessary for the dimensioning of heat exchangers. Reference [8] is recommended for better understanding. For mixed convection and under the effect of mixing caused by secondary currents due to natural convection, the temperature close to the walls changes, as does the bulk temperature; an improvement in heat exchange is obtained on average ( $Nu_{avg}$ ). From a local point of view, depending on the length of the duct, one can have areas with a very high exchange rate, while others are at degraded rate. The first are those where the less hot fluid is located (at the bottom for a horizontal pipe) and vice versa for the second. Sometimes, the tangential evolution of the heat exchange rate at different axial positions is determined. One can easily see the difficulty -because of its variation for any tangential position- of determining the  $Nu_{local}$  without much interest, and the average one (obtained from local  $Nu(s)$ ) which has more physical meaning. It is noted that some authors were interested to the axial position from which the  $Nu_{avg}$  in mixed convection becomes greater than that of forced convection [1;9-11], described by the critical Cameron number. It is obvious that this length (distance measured from the entry section) decreases with increasing  $Gr$  (or  $Ra$ ).

To make the work clearer, the use of nearby works is essential. In addition, and the fact that the mixed convection mode results from the association of forced and natural convection, certain works deemed beneficial are recommended. For the case of *forced convection*, the flow of a nanofluid in an annular space formed by two horizontal ellipses, is treated in [12]. The inner tube is under imposed heat flux and the outer tube is under low temperature. Four types of nanoparticles were assumed for different sizes and concentrations. A  $Re$  ranging from 200 to 1000 was assumed. The results show the increase in heat exchange with  $Re$  and  $\phi$  (volume concentration of nanoparticles), while it decreases strongly, then slightly with the size of the nanoparticles. A rich work but for two cylindrical tubes under imposed flux is carried out in [13]. The effects of aspect ratio, heating density ratio, volume concentration in addition to  $Re$  were analyzed. The reader interested in simultaneous (Hydrodynamic and thermal) development -in a single tube- can consult the work in reference [14]. The work focuses on establishment lengths through experimental tests. It is not limited to forced convection, but extends to mixed convection. Close to the same subject, useful correlations were provided in [15-17]. For the case of *natural convection*, and for two concentric horizontal ellipses, under different temperatures, reference [18] treated the effects of  $Ra$  and  $Pr$ . The results show the increase in disturbances and hence the intensity of heat exchange when  $Ra$  and/or  $Pr$  increases. These results remain valid for a Non-Newtonian fluid with a more accentuated degree for the case of a pseudoplastic (shear-thinning) fluid with a low structure

index  $n$  [19-20]. For the same considerations, the work in [21], deals with the effect of changing the dimensions of the interior ellipse and its orientation (horizontal or vertical). The results are provided for different values of  $Gr$  for the case of air ( $Pr=0.70$ ). For a nanofluid confined between two concentric ellipses, reference [22] studied the effects of  $Ra$  and  $\phi$  on heat transfer. The inner ellipse is assumed to be under heat flux, while the outer ellipse is under low temperature. Different results for the isotherm fields, streamlines, as well as the local temperature along the internal ellipse, the local Nusselt as well as the average one are provided in a methodical manner. For the case of *mixed convection* between two concentric cylinders, reference [23] can be cited. In this work, the authors considered various nanofluids as heating fluids. The inner cylinder is assumed to be insulated, while the exterior is under uniform heat flux. The results show the ameliorative effects of  $Gr$  and  $\phi$ . Noting that a  $Re=800$  and  $Pr=6.2$  were taken for a total length equal to  $100 \times D_h$ . It seems important to note that this work is the successor of many others dealing with the effect of nanoparticle shapes, types,... but in a single tube pipe [24-26]. For an inclined tube with a circulating Newtonian fluid, the work in [27] can be viewed. Note that the situation of natural convection, where a rotation is imposed to the walls, is assumed to be mixed convection. No interest to publications working on this subject was given. The same applies to vertically oriented pipes. For a material exhibiting a phase change, reference [28] is recommended.

According to the consulted works, it can be said that the case of mixed convection in a cylindrical annular space has not benefited from sufficient number of studies. The case with an elliptical passage section even less. For this purpose, in our work, several forms of the passage section (09 in total) are proposed, recalling that their choice is not arbitrary. These forms were considered suitable to remedy the problem of thermal stratification in addition to that of the slowing down of the main flow at the top of the annular space, following the results obtained in [6]. For  $Re$ , a single value equal to 100 is considered. The same goes for the Prandtl number ( $Pr=100$ ). These values are close to those encountered when heating food products. For the Grashof number ( $Gr$ ), a wide range going from 0 (forced convection) to  $5 \times 10^{+5}$  (strong mixed convection) are considered in order to clearly illustrate the formation and the progression of thermal stratification and therefore clearly see the geometric effect. As the practical problem is of the Graetz type (thermal development only), an insulated primary pipe is placed with the aim of establishing the dynamic regime quietly. More details will be presented in the next section.

## 2. PROBLEM DESCRIPTION

The present work deals with thermal development in a mixed convection situation along a horizontal annular duct. The annular space is formed by two concentric ellipses (Figure 1). The two walls are under uniform and equal heat flux densities ( $\phi$ ). The dynamic regime is assumed to be fully developed at the entrance of the

heating zone. For this, a pipe insulated from its two walls is placed before the heating zone. For a  $Re=100$ , a length  $L_D=Re \times D_h$  is taken as sufficient for the dynamic development. The heated zone is spread over a length  $L_{th}=Re \times Pr \times D_h$ , knowing that a  $Pr=100$  is considered. About how these lengths were chosen, see [7]. Concerning the Grashof number ( $Gr$ ), values ranging from 0.0 to  $5.0 \times 10^{+5}$  are considered. It should be noted that the physical properties are assumed to be constant except for density, where Boussinesq hypothesis is adopted. In addition, the case of two cylinders (a cylinder is an ellipse with equal small and big diameters), is studied first and will serve as a control (base) case to well see the geometric influence on the thermal distribution in the section. The values of  $Re$  and  $Gr$  are calculated with the velocity and the hydraulic diameter of the control case. The outer tube diameter  $D_o$  is taken equal to 0.1m and the inner one  $D_i=0.05m$  ( $D_h=D_o-D_i$ ). Consequently, and in order to keep as much as possible the same section area of the annular passage section for all cases, the diameters of the ellipse, small ( $D_{el-s}$ ) and big ( $D_{el-b}$ ) are changed so as to always have the value of the diameters of the control case. That is,  $D_o=(D_{oel-s}+D_{oel-b})/2$  and  $D_i=(D_{iel-s}+D_{iel-b})/2$ .

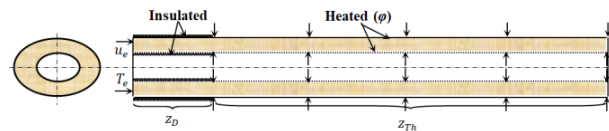


Figure 1. Graphical diagram of the studied problem

The flow is assumed to be laminar and stationary throughout the duct. Axial diffusion is negligible ( $Pe \gg 1$ ). With all assumptions considered, the dimensionless equations of the problem are:

Continuity equation

$$U \frac{\partial U}{\partial X} + V \frac{\partial V}{\partial Y} + W \frac{\partial W}{\partial Z} = 0 \quad (1)$$

X-Momentum equation

$$U \frac{\partial U}{\partial X} + V \frac{\partial U}{\partial Y} + W \frac{\partial U}{\partial Z} = -\frac{\partial P}{\partial X} + \frac{1}{Re} \left( \frac{\partial^2 U}{\partial X^2} + \frac{\partial^2 U}{\partial Y^2} \right) \quad (2)$$

Y-Momentum equation

$$U \frac{\partial V}{\partial X} + V \frac{\partial V}{\partial Y} + W \frac{\partial V}{\partial Z} = -\frac{\partial P}{\partial Y} + \frac{1}{Re} \left( \frac{\partial^2 V}{\partial X^2} + \frac{\partial^2 V}{\partial Y^2} \right) + \frac{Gr}{Re^2} \theta \quad (3)$$

Z-Momentum equation

$$U \frac{\partial W}{\partial X} + V \frac{\partial W}{\partial Y} + W \frac{\partial W}{\partial Z} = -\frac{\partial P}{\partial Z} + \frac{1}{Re} \left( \frac{\partial^2 W}{\partial X^2} + \frac{\partial^2 W}{\partial Y^2} \right) \quad (4)$$

Energy equation

$$U \frac{\partial \theta}{\partial X} + V \frac{\partial \theta}{\partial Y} + W \frac{\partial \theta}{\partial Z} = \frac{1}{Pe} \left( \frac{\partial^2 \theta}{\partial X^2} + \frac{\partial^2 \theta}{\partial Y^2} \right) \quad (5)$$

where:  $Re$ , Reynolds number;  $Pe = Re \times Pr$ , Peclet number; and  $Gr$ , Grashof number.

The following variables were used for scaling the previous equations:

$$X = \frac{x}{D_h}; Y = \frac{y}{D_h}; Z_D = \frac{z}{D_h \text{Re}}; Z_{Th} = \frac{z}{D_h \text{Pe}}; R = \frac{r}{D_h};$$

$$P = \frac{p}{\rho u_e^2}; W = \frac{w}{u_e}; U = \frac{u}{u_e}; V = \frac{v}{u_e}; \theta = \frac{(T - T_e)}{\varphi D_h / k} \quad (6)$$

where:  $u, v$ , were the velocity components following  $x, y$  and  $z$  directions respectively.  $p$ , is the pressure,  $T$  the temperature.  $k, D_h$  and  $\varphi$  are the thermal conductivity, the hydraulic diameter and the heat flux density respectively. The subscript  $e$  is for entrance.

### Boundary conditions

$$Z_D = 0 \Rightarrow W = \frac{\text{Re} \cdot \mu}{\rho \cdot D_h}; U = V = 0; \theta = 0$$

$$Z_D = 0 \rightarrow 1 \Rightarrow \underbrace{\left( \frac{(X \cdot D_h)^2}{D_{el-b}^2} + \frac{(Y \cdot D_h)^2}{D_{el-s}^2} \right)}_{\text{walls}} \Big|_{i,o} = 1 \rightarrow \begin{cases} U = V = W = 0 \\ \varphi = 0 \text{ W/m}^2 \end{cases}$$

$$Z_D = 1 \text{ or } Z_{Th} = 0 \Rightarrow \underbrace{W = f(R)}_{\text{Full Develop}}; U = V = 0; \theta = 0$$

$$Z_{Th} = 0 \rightarrow 1 \Rightarrow \underbrace{\left( \frac{(X \cdot D_h)^2}{D_{el-b}^2} + \frac{(Y \cdot D_h)^2}{D_{el-s}^2} \right)}_{\text{walls}} \Big|_{i,o} = 1 \rightarrow \begin{cases} U = V = W = 0 \\ \varphi = 1000 \text{ W/m}^2 \end{cases} \quad (7)$$

$$Z_{Th} = 1 \Rightarrow \frac{\partial U}{\partial Z} = \frac{\partial V}{\partial Z} = \frac{\partial W}{\partial Z} = 0; \frac{\partial}{\partial Z} \left( \frac{\partial \theta}{\partial Z} \right) = 0$$

$$\underbrace{X = 0; Y = -1 \rightarrow +1; Z = 0 \rightarrow Z_D + Z_{Th}}_{\text{Symm plane}} \Rightarrow \frac{\partial}{\partial X} = 0$$

## 3. NUMERICAL SOLUTION

The problem is solved numerically using the finite volume method, following the steps of the SIMPLE algorithm [29]. The symmetry with respect to the vertical plane passing through the centers of the two ellipses, allows working only on half of the duct. A second-order central differencing scheme is used for the diffusive terms, and a second-order up-wind scheme is used for the convective terms. Strong convergence criteria have been imposed, where residuals of  $10^{-6}$  are considered for the equations of motion and that of continuity, while a residual of  $10^{-7}$  is taken for the energy equation.

### 3.1 Mesh study

In order to overcome the errors caused by the numerical resolution without wasting too much time in calculation, an optimal mesh is chosen after tests. The 3D nature of the problem required testing the effect of mesh size in the section and also along the length. For this, initially 80 divisions were taken for each meter of length. Following  $X$  and  $Y$  directions, 20 divisions were taken at first (for each annular space). Subsequently, the number was increased to 30 then to 40. In a second test, the transversal 40 divisions' case was fixed and a refinement according to the length was done by taking 100 divisions for each meter. All the cases were compared each other. For more confidence, a comparison with a more refined mesh of  $50 \times 50$  divisions in the section was done (Figure 2). It can

easily be seen the sufficiency of the  $40 \times 40 \times 100_m$  mesh from the results on the isotherms field and the maximum value of the temperature in the section for a strong  $Gr$ . It should be noted that an equidistant mesh is chosen because of the strong disturbances in the central zone too, due to the recirculation (Figure 3).

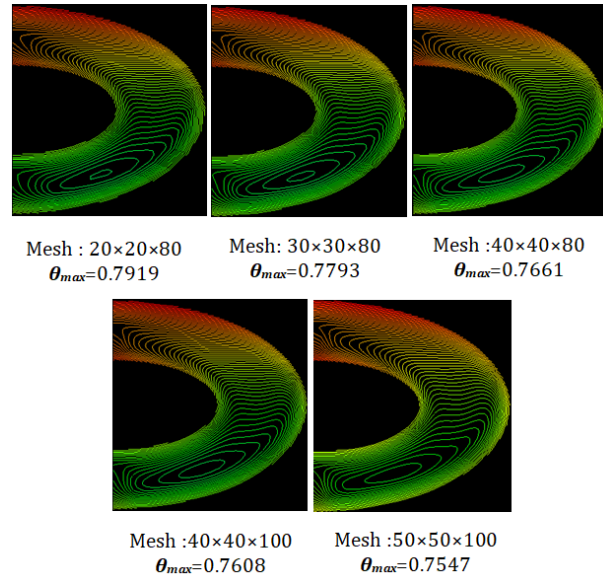


**Figure 2. Mesh effect on temperature field. Case: Two ellipses:  $D_{oel-s}=1.4/D_{oel-b}=2.6; D_{iel-s}=0.6/D_{iel-b}=1.4. Gr=10^{+5}; Re=100; Pr=100$**

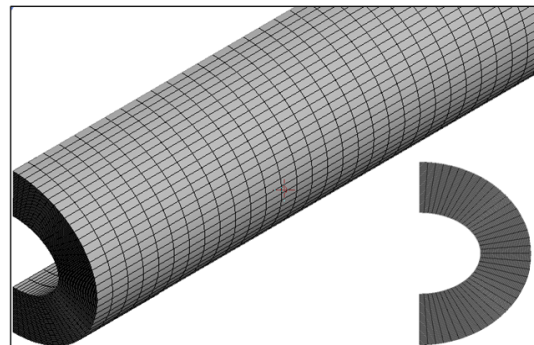


**Figure 3. Optimal mesh. Case: Two ellipses:  $D_{oel-s}=1.8/D_{oel-b}=2.2; D_{iel-s}=0.8/D_{iel-b}=1.2$**

### 3.2 Validations

For this part, a single comparison is presented. It is made with the work in [30], recommended for its scientific richness. The compared case is for mixed convection between two concentric horizontal cylinders with aspect ratio ( $R_o/R_i$ ) equal to 2.0. Both walls are heated to the same heat flux density.  $Re$  is taken equal to 35,  $Pr=557.3$  and  $Gr=6000$ , respectively. The compared result is that of the axial evolution of temperatures on the exterior wall for one angle equal to 0 and the other equal  $\pi$  for a cylindrical duct. The first position is at the very top and the second at the very bottom (on the axis of symmetry). For our considerations, these two positions are for ( $X=0; Y=+1$ ) and ( $X=0; Y=-1$ ), respectively. A total length  $z=125 \times R_o$  is taken. An excellent agreement is easily observed. Another validation can be mentioned for the velocity profile at the establishment in the isolated part, where the profile

of the figure (5. (a)), in the section 4.1(bellow), is exactly that obtained in [13, Figure. 4], and [7, Figure.2] for a Newtonian fluid. The maximum value obtained (1.507)is equal to that obtained by [31, Table.1].

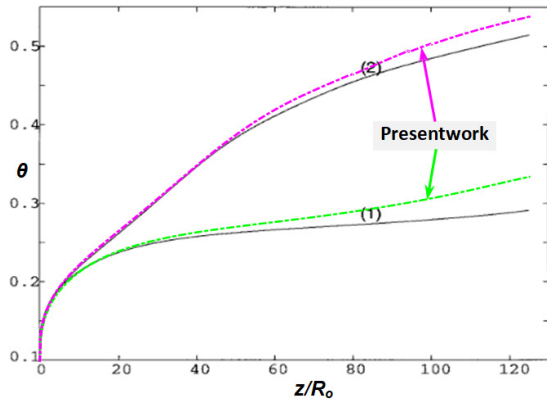


**Figure 4. Present work validation (very bottom (1): - - -;very Top (2): - - -, with reference [30] for the outer wall dimensionless temperature along the duct.  $Re=35$ ;  $Pr=557.3$ ;  $Gr=6000$ ;  $R_o/R_i=2.0$**

#### 4. RESULTS AND DISCUSSION

For a better understanding of the work results, they will be classified into three sections. The first focuses on the dynamic development in the isolated part for a pipe formed by two cylinders. Subsequently, the results along the heated part will be presented, where both the case of forced convection ( $Gr=0.0$ ) and that of mixed convection ( $Gr>0.0$ ) are treated. Full details will be given for this section. The last section is devoted to the geometric effect, where the results for eight (08) annular elliptical sections will be presented. As already mentioned in the introduction, no results for Nusselt number will be presented.

The symmetry in the duct is exploited in the presentation of the results; where one half is devoted to isovelocities, while the other to isotherms. Only the results for the tangential velocity are presented over the entire annular space for better clarity, noting that the legends of the different figures are valid for all the subfigures included. For example, for isotherms along the duct, one can know the values for each position using the same legend. The maximum is therefore the maximum in the total duct and the same for the minimum. In addition, certain subfigures were presented with a black background. It is the background which gives the best clarity after tests.

##### Dynamic profile for concentric cylinders

In this first section, some details for the dynamic development from the entrance of the isolated zone ( $Z_D=0.0$ ) to its exit ( $Z_D=1.0$ ) are presented. For the other geometries, the process is the same, indicating that the geometric modification generates radial and azimuthal modifications in the velocity profile, which can be summarized by a stronger acceleration (compared to the uniform entry velocity) in the narrow zones, and the opposite in widened ones. Reference [31] offers diverse results regarding the geometric effect on the velocity and the friction coefficient.

The results for the velocity profile are shown in figure (5). Subfigure (a) is for the radial evolution of the axial velocity for different axial positions, starting from the uniform inlet velocity equal to 1.0. Progressively and due to friction on the walls, the velocity is zero at the walls, and by mass conservation, the flow accelerates in the middle. The viscosity is the cause of these braking and acceleration. After a certain distance, the profile becomes quasi-parabolic (the maximum is not halfway between the two walls for annulus). After this distance, the profile stops changing and one speaks of dynamic (or hydrodynamic) establishment. In subfigure (b), the velocity profile at the radial position of the maximum from the inlet to the exit is plotted. One can easily see the establishment zone described by horizontal stability. The distance from the entrance to the  $Z$  corresponding to the start of the horizontal evolution' position is the dynamic length ( $Z_D$ ). This length increases with  $Re$  and vice versa. Furthermore, one can easily see that for  $Re=100$ , assumed in our work, the dynamic regime can be considered fully developed at the entrance of the heated part. In subfigure (c), the isovelocities in the ( $X,Y$ ) plane for  $Z_D=1.0$  are plotted. The velocity is described by concentric circles with a minimum equal to 0 at walls and a maximum in the middle.

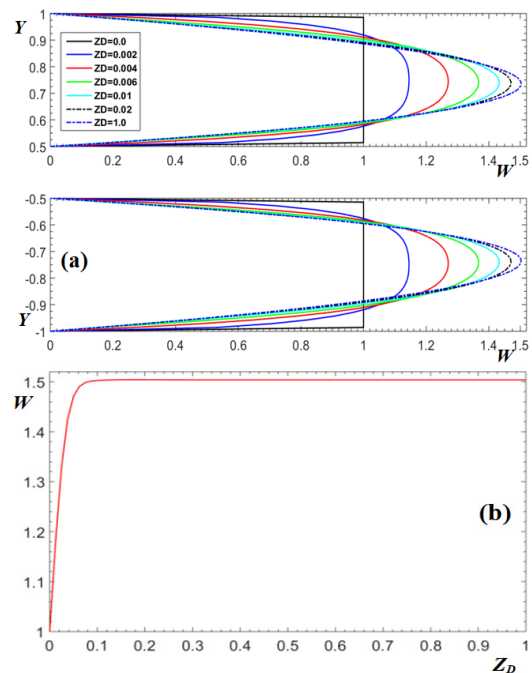


**Figure 5. Velocity profiles in the isolated part. (a):  $W(Y)$  at different axial positions; (b): Velocity at the  $Y$  line of  $W_{max}$ ; (c): Isovelocities in the ( $X,Y$ ) plane at the exit of the isolated part ( $Z_D=1$ ).  $Re=100$**

## Mixed convection for cylindrical tubes

This part focuses on the thermal development for the case of a duct formed by two concentric cylinders. The aspect ratio ( $D_o/D_i$ ) equals 2. Reynolds number is taken equal to 100 and the Prandtl number equals 100. A Grashof number ranging from 0.0 to  $5.0 \times 10^{+5}$  is considered. The results for the velocity (left half) and temperature (right half) fields are shown in figure (6). Six axial positions are considered, starting from a position close to the entrance of the heating zone ( $Z_{Th}=0.1$ ) to its exit ( $Z_{Th}=1.0$ ), passing through  $Z=0.2, 0.4, 0.6$  and  $0.8$  respectively.

For the case of forced convection ( $Gr=0.0$ ), the flow already established does not undergo any modification. The velocity field shows concentric circles with zero velocities at walls and progressively increasing moving towards the middle (review section 4.1). The maximum velocity for annular pipes is not halfway between the two walls and changes with the aspect ratio [7; 31-32]. The temperature field presents a quiet progressive change which is characterized by the penetration of heat from walls towards the middle of the annular space. The initially blue field ( $\theta=0.0$ ) begins by becoming red close to the walls, and little by little the change in blue color reaches the entire annular space, which becomes green, yellow and finely orange, indicating the increase in temperature along of duct. It is obvious that the greatest temperatures are near the walls, in particular the exterior one of the largest diameter which allows more thermal heat flux to be introduced. In summary, the temperature field also presents concentric circles.

When  $Gr$  becomes non-zero, this implies that the density of the fluid changes with temperature. For a heating case, it decreases. Therefore, the hot fluid becomes lighter and moves upward. Since the hot zones are the walls, this is where the density changes first. The closed geometric shape generates an ascending azimuthal movement close to the walls, while the continuity in the section generates a downward movement in the space in between. The results in the figure (7) for the tangential component of velocity clearly show what has been said. Comparing the three subfigures at  $Z_{Th}=0.1$  (near the entrance of the heated zone),  $0.6$  (in the middle) and  $1.0$  (at the exit) respectively, one can see that the intensity of the ascending and descending currents are stronger near the entrance than far from it. This is explained by the fact that close to the entrance, the fluid is still cold and the slightest change in its temperature will cause a clear decrease in its density and hence the tangential velocity; while after a certain distance, the change in temperature between the walls and the fluid becomes less strong due to thermal mixing. Therefore, a reduction in intensity of the tangential movement is observed. It should be recalled that this difference will stabilize once full thermal development is reached [3]. In addition, close to the entrance, more intensity near the outer wall than the inner wall is recorded, due to stronger heating as a consequence of the greater amount of heat entering the outer wall of bigger surface. This result becomes unclear after a certain distance with increasing fluid temperature and mixing in the section.

The ascending-descending movement directly influences the main forced convection movement. The circular shapes gradually disappear along the pipe, and an increasingly disturbed shape results (Figure 6 *b*, *c*, and *d*). It is obvious that the value of  $Gr$  has an importance in the degree of disturbance. The results show that case  $Gr=10^{+4}$  presents a low disturbance, while the one with  $Gr=5.0 \times 10^{+5}$  shows the highest disturbance. The case  $Gr=10^{+5}$  is clearly disturbed, without being strongly disturbed. It can easily be seen that the disturbances start earlier when  $Gr$  increases. The ascending hot fluid opposes the main flow at the top; so, one observes a deceleration of the flow at the top. By continuity in the section, acceleration will take place at the bottom. Recalling that, a strong deceleration degrades the convective heat exchange and tends it towards the conductive mode. Precautions are necessary for strong  $Gr$ . On the thermal field, one can see the effect of the hot ascending flow and the less hot one descending in the accumulation of the hot fluid at the top and the other at the bottom, hence the thermal stratification. The comparison -as an example- of the results for  $Z_{Th}=1.0$  for the three non-zero values of  $Gr$ , shows the stratification for all these values; but the difference ( $\Delta\theta$ ) between the highest temperature and the lowest clearly increases with  $Gr$ .

As the maximum velocity is at the bottom ( $X=0; Y(-)$ ) and the minimum is at the top ( $X=0; Y(+)$ ), the velocity profile for the six (06)  $Z$  positions already considered is plotted, in addition to that at the entrance of the heated part ( $Z_{Th}=0.0$ ). The results for  $Gr=0.0$  do not change and the profile at the input remains the same until the output. The changes for  $Gr=10^{+4}$  were very small and were not presented. Those for  $Gr=10^{+5}$  and  $5.0 \times 10^{+5}$  are shown in figure (8). For  $Gr=10^{+5}$ , the effect of slowing down at the top and accelerating at the bottom becomes clear for  $Z_{Th}=0.2$  (For the positions shown), which reflects that the azimuthal movement caused by natural convection has intensified. The maximum velocity that was 1.507 at the inlet decreases to 1.35. While at the bottom it increases approximately to 1.63 then a small deceleration is observed far from the input ( $Z_{Th}=0.8$  and  $1.0$ ) up to 1.58. This is explained by the weakening of the azimuthal movement away from the entrance. For this value of  $Gr$ , the deceleration remains weak overall.

For  $Gr=5.0 \times 10^{+5}$ , the acceleration at the bottom and the deceleration at the top start too early with strong degrees. Little by little, the opposite phenomena results, as a consequence of the diffusion of disturbances throughout the annular space. The flow regenerates the velocity at the top and the reverse at the bottom. But it should be noted that despite this gain, the velocity remains very low compared to the inlet velocity. It goes from 1.507 to 0.8 ( $<U_e$ ), then rises to 1.0 ( $=U_e$ ). Referring to figure (6) shows the widening of the low velocity zone and therefore the promotion of the conduction heating mode over a larger space.

## 4.2. Mixed convection for elliptical tubes

In this last section, the geometric effect of the annular cross-section is treated. In addition to the base case (two

cylinders), eight (08) geometric shapes are assumed. First, an interior cylinder for an exterior ellipse. In this case too, two sizes are assumed for the ellipse ( $D_{oel-s}/D_{oel-b}$ ). Subsequently, an exterior cylinder and an interior ellipse. Two different sizes are assumed for the ellipse ( $D_{iel-s}/D_{iel-b}$ ). Finally, two ellipses (interior and exterior) where four sizes were assumed. A care is taken for the choices to keep the annular space wide to avoid the great rapprochement of the walls which favors the conductive mode by breaking down the flow under friction effect. The results for the dynamic and thermal fields are shown in figure (9). Because the ellipses are horizontal, only results from  $Z_{Th}=0.2$  are presented, in order to allow sufficient space for the sub-figures and respect the page size. Furthermore,  $Z_{Th}=0.1$  is very close to the entrance and therefore ignoring it does not cause a real inconvenience.

The first result that can be noted is the modification in the velocity field under the geometric effect. The flow is accelerated in the wide zones and decelerated in the narrow zones. Therefore, better heat exchange will take place in the first zones. In addition, narrow areas are described by walls close to each other. Therefore the thickness of the layers of fluid between them is small and their heating will be faster. A strong decrease in density, and therefore more intensity of the azimuthal flow (Case 3 and case 5). These areas experience more braking of the main flow. When this rapprochement is Vertical (Case 3), the widening above the low narrow zone -at high axial velocity- serves as a mixing zone where the small rising hot quantities will be mixed with the large less hot quantities above.

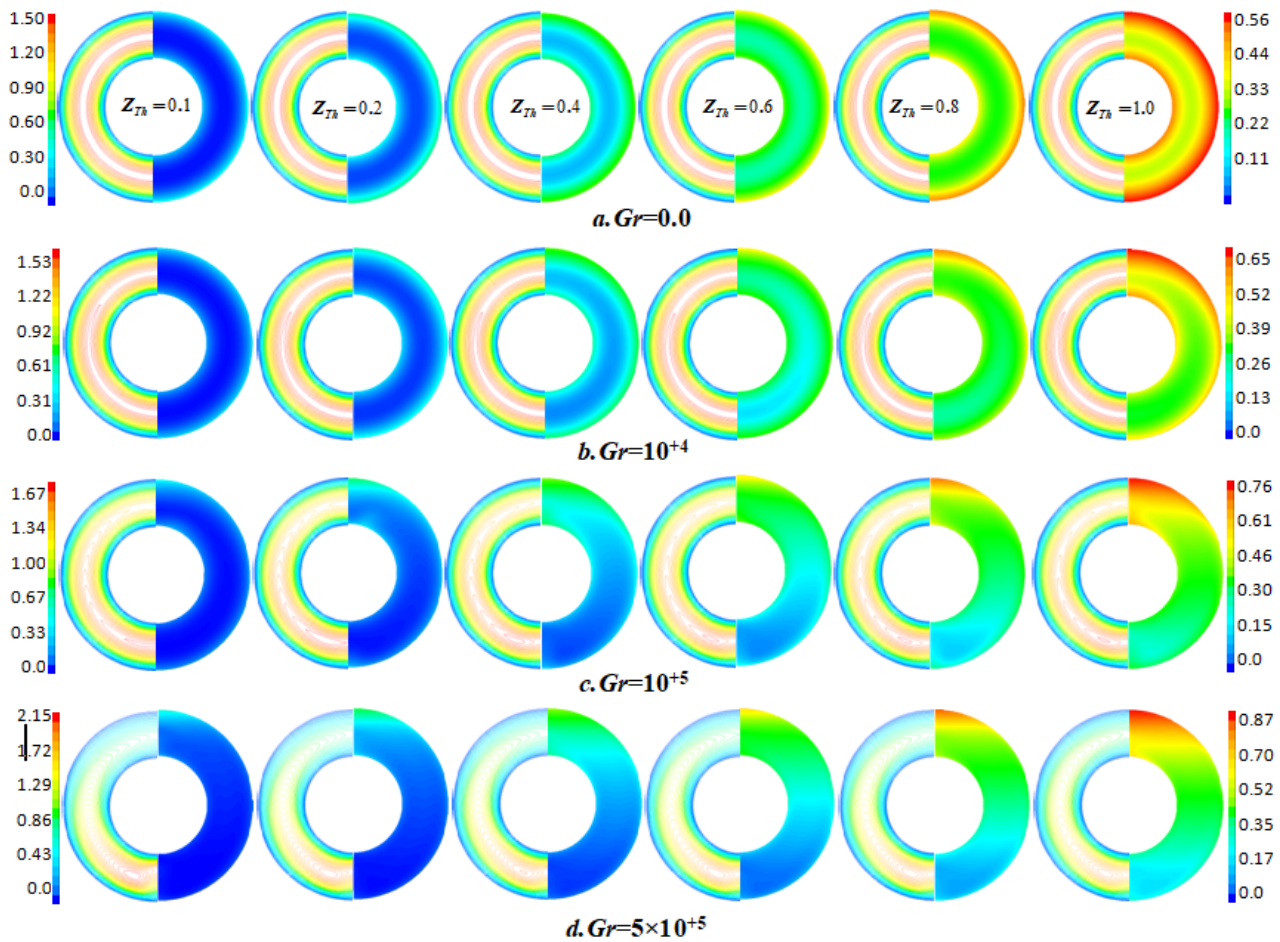


Figure 6. Isovelocities(Left half) and isotherms (Right half) at different axial positions for different  $Gr$  values.  $Re=100$ ;

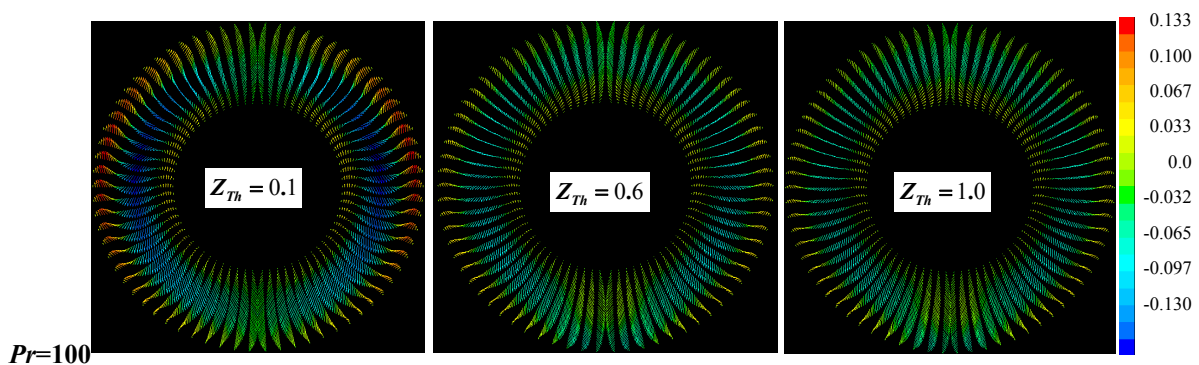


Figure 7. Tangential velocity at different axial positions.  $Gr=10^5$ ;  $Re=100$ ;  $Pr=100$ .

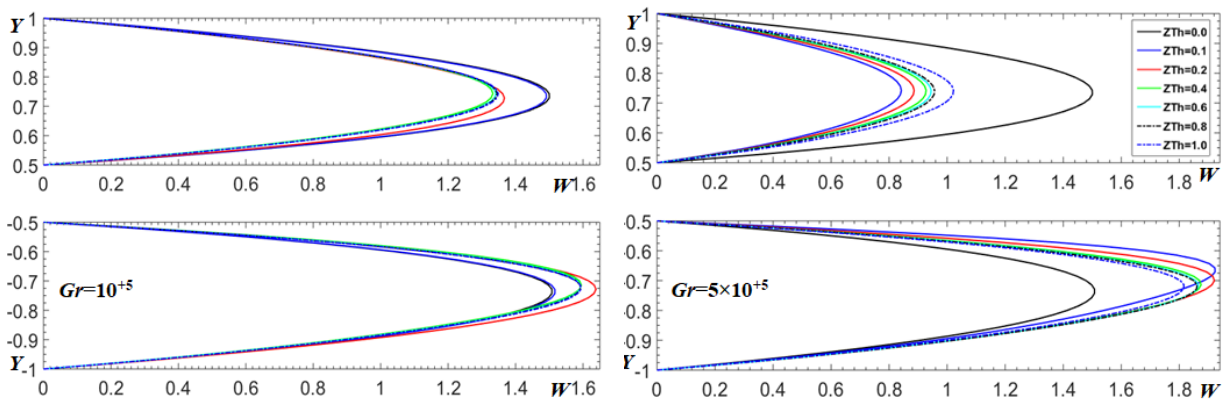


Figure 8. Velocity profile at  $X=0$  (Top and Bottom) at different axial positions and  $Gr$  number.  $Re=100$ ;  $Pr=100$

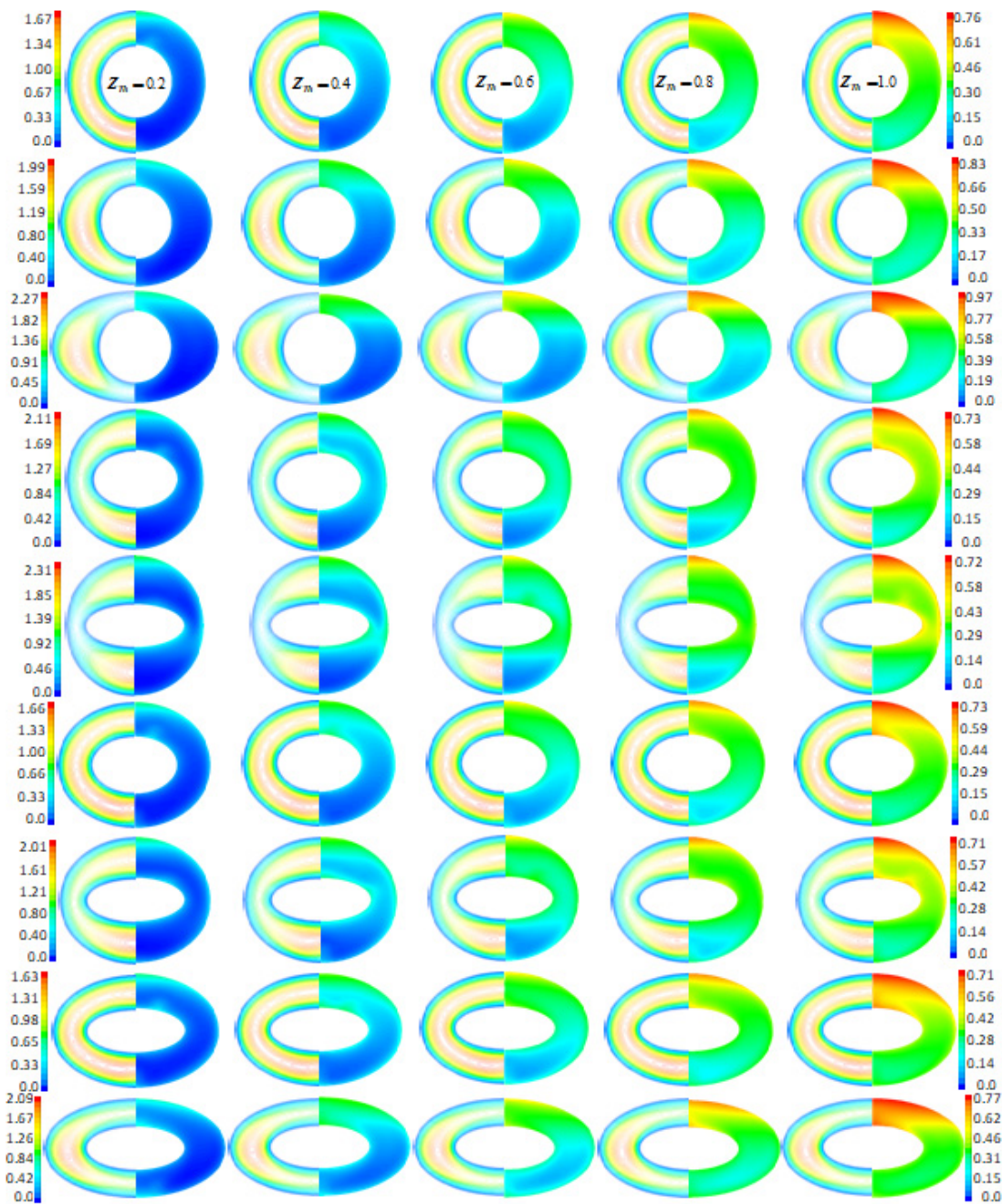
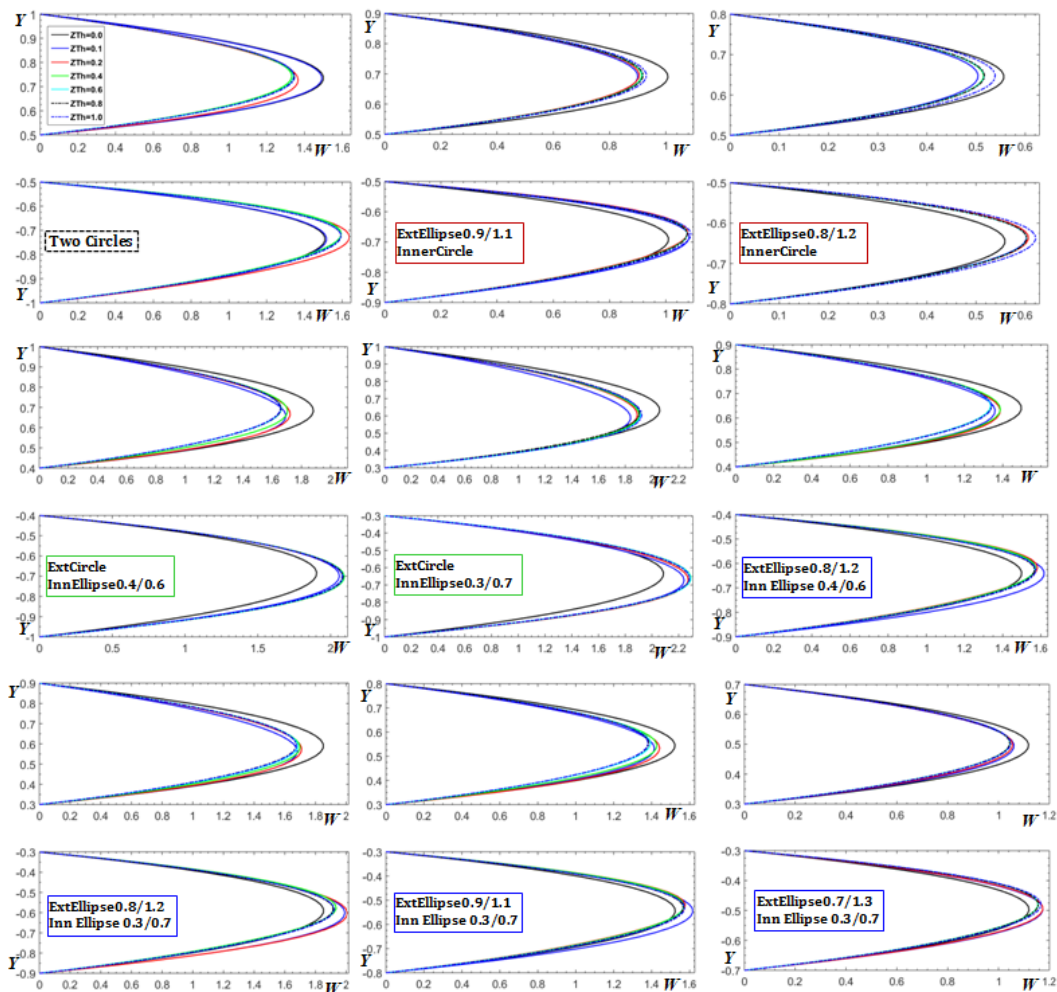


Figure 9. Isovelocities (Left half) and isotherms (Right half) at different axial positions for the nine (09) supposed geometries.  $Gr=10^5$ ;  $Re=100$ ;  $Pr=100$ . Cases from top to bottom: 1: Ex-C/In-C; 2: Ex-EI (0.8/1.2)/In-C; 3: Ex-EI (0.9/1.1)/In-C; 4: Ex-C/In-EI(0.4/0.6); 5: Ex-C/In-EI (0.3/0.7); 6: Ex-EI (0.9/1.1)/In-EI (0.4/0.6); 7: Ex-EI (0.9/1.1)/In-EI (0.3/0.7); 8: Ex-EI (0.8/1.2)/In-EI (0.3/0.7); 9: Ex-EI (0.7/1.3)/In-EI (0.3/0.7)



**Figure 10. Velocity profile Top ( $Y=+1$ ) and Bottom ( $Y=-1$ ) of the section at different axial positions for the nine (09) considered geometries.  $Gr=10^{+5}$ ;  $Re=100$ ;  $Pr=100$**

Much of the stratification is caused by rapprochement at the top. Gradually a hot fluid accumulation at higher temperature compared to the case with two cylinders is recorded. In the other case, when the approximation is horizontal (Case 5), narrow zones are on (and close to) the plane  $Y=0$ . A reduction in the quantity of the hot ascending fluid will take place. In addition, the widening at the bottom cools the ascending fluid close to the heated walls. As a result, a weakening in the stratification will take place by reducing the quantity of the hot ascending fluid without forgetting the further mixing in the upper part as well. Thus, the highest temperature recorded is lower than that of the base case.

For the case of two ellipses, the fluid heating trajectories next to the walls are spread out horizontally. That is, their rejoining the upper zone is delayed. In addition, the similar shapes of the two walls keep a considerable space between them and therefore the reduction in velocity by rapprochement is avoided, which will induce a mixing between hot and cold currents over greater distances. This will reduce the levels of maximum temperatures reached and increase those of minimum temperatures (by mixing). The two cases 7 and 8 show the small differences in temperature between the top and the bottom in the section. In addition, Case 8 presents more homogeneity in the temperature field and also that of the velocity, which is

a very important characteristic. Case 9 is not good but better than cases 1 to 5 by comparing the temperature difference ( $\Delta(\theta)$ ) between the maximum and minimum from the figure's legends.

As done for the case of two cylinders, the velocity profiles ( $W(Y)$ ), top ( $X=0, Y=(+)$ ) and bottom ( $X=0, Y=(-)$ ) are plotted (Figure 10) for the same axial positions chosen for figure (8). The objective is to see the levels of acceleration at the bottom and deceleration at the top when the disturbances by natural convection reach their highest intensity. One can easily see that the cases with two ellipses prevent blocking at the top and thus maintain a good convective heat exchange, in particular for cases 8 and 7. This result in addition to that of the clearer homogeneity, allows us to recommend this type of annular space compared to the classic one with confidence.

## 5. CONCLUSIONS

This numerical work allowed us to conclude that:

- The increase in the intensity of natural convection ( $Gr \uparrow$ ), disturbs the dynamic and thermal fields. Thermal stratification between the top and bottom of a section results. These disturbances are increasingly stronger and start earlier when  $Gr$  is larger.
- An acceleration at the bottom of the section and a deceleration at the top are recorded. A tendency for conductive heat transfer will take place at the top with

high temperatures which risk denaturing the heating fluid.

- The use of an elliptical shape instead of a circular one for the passage section modifies the velocity field and also that of temperature. Among the nine (09) assumed cases, the case with two ellipses offers better homogeneity in the thermal field and also in the dynamic field. The case of an interior ellipse and an exterior circle comes next, then the classic case and finally the opposite case.

- From the results obtained, it is recommended changing annular pipes with circular cross-section by others with elliptical one. This not only reduces thermal stratification, resulting in a net economic gain, but also makes it possible to reduce the sizes (lengths) of the heat exchangers given the improvement in heat penetration to the core of the annular space by the better distributed secondary currents.

## REFERENCES

- [1] Nouar, C., Benaouda-Zouaoui, B., Desaubry, C.: Laminar mixed convection in a horizontal annular duct. Case of thermo dependent non-Newtonian fluid, *Eur. J. Mech. Fluids*, Vol. 19, No. 3, pp. 423-452, 2000.
- [2] Saadjan E.: *Transport phenomena and their numerical resolutions* (in French), Second ed., Polytechnica, Paris, 1998.
- [3] Horimek A.: *Laminar flow in mixed convection in an eccentric horizontal annular pipe -case of a thermodependent pseudoplastic fluid-*, PhD thesis (in French), Mechanical Engineering institute, Blida 1 University, Algeria, 2014.
- [4] Ait-Messaoudene, N., Horimek, A., Nouar C., Benaouda-Zouaoui B.: Laminar mixed convection in an eccentric annular horizontal duct for a thermo-dependent non-Newtonian fluid, *Int. J. Heat Mass Transf.*, Vol. 54, No. 19-20, pp. 4220-4234, 2011.
- [5] Horimek, A. and Ait-Messaoudene, N.: Laminar flow for a Newtonian thermodependent fluid in an eccentric horizontal annulus, in: Driss, Z., Necib, B. and Zhang H-C. (Ed.): *CFD Technics and Thermo-Mechanics Applications*, Springer, Germany, pp.151-160, 2018.
- [6] Horimek, A., Farhat, A. and Ait-Messaoudene, N.: Natural convection between two concentric ellipses with different imposed temperatures, in: Driss, Z. (Ed.): *Mechanical Engineering Technologies and Applications, Vol. 2*, Publisher: Bentham Science Publishers, Sharjah, U.A.E, pp. 105-127, 2023.
- [7] Horimek, A., Ait-Messaoudene, N., Aich, W., Aichouni, M., Kolsi, L. and Ghernaout J.: Laminar forced convection of a pseudoplastic thermo-dependent fluid in an annular horizontal duct, *Arab Gulf J. Sci. Res.*, Vol. 33, No. 4, pp. 125-137, 2015.
- [8] Horimek, A., Abed, S. and Ait-Messaoudene, N.: Non-newtonian pseudoplastic fluid flow and heat transfer inside a horizontal duct: New correlations, in: Driss, Z. (Ed.): *Mechanical Engineering Technologies and Applications, Vol. 3*, Bentham Science Publishers, Sharjah, U.A.E, pp. 72-88, 2023.
- [9] Nazrul, I., Gaitonde, U.N. and Sharma, G.K.: Mixed convection heat transfer in the entrance region of horizontal annuli, *Int. J. Heat Mass Transf.*, Vol. 44, No. 11, pp. 2107-2120, 2001.
- [10] Om, N.I. and Mohammed, H.A.: Numerical study of mixed convection through horizontal duct utilizing Al<sub>2</sub>O<sub>3</sub>, *Appl. Mech. Mater.*, Vol. 819, pp. 111-116, 2016.
- [11] Salman, Y.K., Jalil J.M and Khudheyer, A.F.: Experimental Study of Mixed Convection Heat Transfer to Thermally Developing Air Flow in a Horizontal Rectangular Duct, *Int. J. Comput. Appl.*, Vol. 174, No. 25, pp. 44-53, 2021.
- [12] Dawood, H.K., Mohammed, H. and Munisamy, K.M.: Heat transfer augmentation using nanofluids in an elliptic annulus with constant heat flux boundary condition, *Case Stud. Therm. Eng.*, Vol. 4, pp. 32-41, 2014.
- [13] Izadi, M., Behzadmehr, A., Behzadmehr, A. and Jalali-Vahida, D.: Numerical study of developing laminar forced convection of a nanofluid in an annulus, *Int. J. Therm. Sci.*, Vol. 48, No. 11, pp. 2119-2129, 2009.
- [14] Horimek, A., Oueld-M'barek, A. and Sadeddine, M.: Effect of an inward-facing baffle on the laminar forced convection heating along a cylindrical horizontal pipe for different nanofluids, *Heat Transf. Res.*, Vol. 55, No. 15, pp. 57-78, 2024.
- [15] Laith, J.H., Fouad, A.S. and Bassim, M.M.: CFD modeling of laminar flow and heat transfer utilizing Al<sub>2</sub>O<sub>3</sub>/water nanofluid in a finned-tube with twisted tape, *FME Trans.*, Vol. 47, No. 1, pp. 89-100, 2019.
- [16] Rajesh K.P., Sivasubramanian, M. and Uthayakumar, M.: Numerical investigation of forced convection heat transfer from square cylinders in a channel covered by solid wall-conjugate situation, *FME Trans.*, Vol. 45, No. 1, pp. 16-25, 2017.
- [17] Everts, M., Meyer, J.P.: Laminar hydrodynamic and thermal entrance lengths for simultaneously hydrodynamically and thermally developing forced and mixed convective flows in horizontal tubes, *Exp. Therm. Fluid Sci.*, Vol. 118, 110153, 2020.
- [18] Bouras, A., Djezzar, M. and Ghernoug, C.: Numerical Simulation of Natural Convection between two elliptical cylinders: Influence of Rayleigh number and Prandtl number, *Energy Procedia*, Vol. 36, pp. 788-797, 2013.
- [19] Turan, O., Lai, J., Poole, R.J. and Chakraborty, N.: Laminar natural convection of power-law fluids in a square enclosure submitted from below to a uniform heat flux density, *J. Nonnewton. Fluid Mech.*, Vol. 199, pp. 80-95, 2013.
- [20] Horimek, A.: Non-Newtonian natural convection cooling of a heat source of variable length and position placed at the bottom of a square cavity, *Therm. Sci.*, Vol. 27, No. 5B, pp. 4161-4178, 2023.

- [21] Djezzar, M., Chaker, A. and Daguene, M.: Numerical study of bidimensional steady natural convection in a space annulus between two elliptic confocal ducts influence of the internal eccentricity, *Rev. Energ. Ren.*, Vol. 8, pp. 63-72, 2005.
- [22] Tayebi, T., Chamkha, A.J. and Djezzar, M.: Natural convection of CNT-water nanofluid in an annular space between confocal elliptic cylinders with constant heat fluxes on inner wall, *IJST-T Mech. Eng.*, Vol. 26, No. 5, pp. 2770-2783, 2019.
- [23] Benkhedda, M., Bensouici, F. and Boufendi, T.: Parametric study of nanoparticles effects on convective heat transfer of nanofluids in a heated horizontal annulus, *J. Nano Res.*, Vol. 70, pp. 81-100, 2021.
- [24] Benzeggouta, O., Boufendi, T. and Touahri, S.: Comparative study of fluid flow and heat transfer between usual fluids and nanofluids in a heated horizontal pipe, *J. Therm. Sci. Technol.*, Vol. 13, No. 2, 17-00366, 2018.
- [25] Khemici, M., Boufendi, T. and Touahri, S.: Numerical study of developing laminar mixed convection in a heated annular duct with temperature dependent properties, *Therm. Sci.*, Vol. 23, No. 6A, pp. 3411-3423, 2019.
- [26] Benkhedda, M., Boufendi, T. and Touahri, S.: Laminar mixed convective heat transfer enhancement by using Ag-TiO<sub>2</sub>-water hybrid nanofluid in a heated horizontal annulus, *Heat Mass Transf.*, Vol. 54, No. 1, pp. 2799-2814, 2018.
- [27] Ibrahim E.S., Sattar A. and Karamallah, A.A.: Effect of Al<sub>2</sub>O<sub>3</sub>/CuO hybrid nanoparticles dispersion on melting process of PCM in a triplex tube heat storage, *FME Trans.*, Vol. 51, No. 4, pp. 606-626, 2023.
- [28] Bouhezza, A., Kholai, O., Boudebous, S., Nemouchi, Z.: Mixed convection heat and mass transfer in inclined circular ducts, *Heat Transf. Res.*, Vol. 44, No. 2, pp. 163-193, 2013.
- [29] Patankar, S.V.: *Numerical Heat Transfer and Fluid Flow*, Hemisphere, Washington, DC, 1982.
- [30] Nouar, C.: Numerical solution for laminar mixed convection in a horizontal annular duct: temperature-dependent viscosity effect, *Int. J. Numer. Methods Fluids*, Vol. 9, No. 7, pp. 849-864, 1999.
- [31] Dos Santos Júnior, V.A., Barbosa de Lima, A.G., Rodrigues de Farias, N.S., Gomes, I.F. and Cunha Teixeira, J.D.: Laminar fluid flow in concentric annular ducts of non-conventional cross-section applying GBI method, *Res. Soc. Dev.*, Vol. 10, No. 1, e10710111547, 2021.
- [32] Bird, R.B., Armstrong, R.C. and Hassager, O.: *Dynamics of polymeric liquids, Vol.1, Fluid mechanics*, Second ed., Wiley, New-York, 1987.

## NOMENCLATURE

|       |  |
|-------|--|
| $c_p$ | Specific heat, [ $J \cdot Kg^{-1} \cdot ^\circ C^{-1}$ ] |
| $D_h$ | Hydraulic diameter, [ $m$ ]                              |
| $g$   | Gravity acceleration, [ $m \cdot s^{-2}$ ]               |

|           |   |
|-----------|---|
| $Gr$      | Grashof number  |
| $k$       | Thermal conductivity, [ $J \cdot s^{-1} \cdot m^{-1} \cdot ^\circ C^{-1}$ ] |
| $L$       | Length, [ $m$ ]   |
| $p$       | Pressure, [ $Kg \cdot m^{-1} \cdot s^{-2}$ ]                                |
| $Pr$      | Prandtl number  |
| $Pe$      | Peclet number   |
| $Re$      | Reynolds number   |
| $T$       | Temperature, [ $^\circ C$ ]   |
| $u, v, w$ | $x, y$ and $z$ velocity components, respectively [ $m \cdot s^{-1}$ ]       |
| $x, y, z$ | Horizontal, vertical and axial coordinate, respectively [ $m$ ]             |

## Greek symbols

|           |  |
|-----------|--|
| $\rho$    | Fluid density, [ $Kg \cdot m^{-3}$ ]                 |
| $\theta$  | Dimensionless temperature                            |
| $\beta$   | Thermal expansion coefficient, [ $1/^\circ C$ ]      |
| $\mu$     | Viscosity, [ $Kg \cdot m^{-1} \cdot s^{-1}$ ]        |
| $\varphi$ | Heat flux density, [ $J \cdot s^{-1} \cdot m^{-2}$ ] |

## Subscripts

|       |               |
|-------|---------------|
| $b$   | Big           |
| $D$   | Dynamic       |
| $e$   | Entry         |
| $el$  | Ellipse       |
| $i$   | Inner         |
| $o$   | Outer         |
| $s$   | Small         |
| $Th$  | Thermal       |
| $oel$ | Outer ellipse |
| $iel$ | Inner ellipse |

## ЛАМИНАРНА МЕШОВИТА КОНВЕКЦИЈА У ПРСТЕНАСТОМ ХОРИЗОНТАЛНОМ ЕЛИПТИЧНОМ КАНАЛУ

А. Хоримек, Н. Аит-Месаодене

У овом раду, нумерички се проучава загревање ламинарном мешовитом конвекцијом дуж хоризонталног канала, формираног од две концентричне елиптичне цеви под једноликим и једнаким топлотним флуксевима, користећи методу коначних запремина. Рад се фокусира на геометријски ефекат пресека пролаза канала, где је предложено девет случајева, почевши од случаја са два цилиндра, затим случај унутрашњи цилиндар/спољашња елипса, затим супротно и коначно случај са две елипсе.  $Re=100$  је узето за  $Pr=100$ , док се претпоставља  $Gr$  у распону од 0,0 до  $5,0 \times 10^5$ . Резултати за основни случај за кружни попречни пресек - који се среће у прехрамбеној индустрији - показују након одређене удаљености од улаза формирање термичке стратификације између врха и дна пресека где топлији флуид ризикује да буде денатурисан, са јаким успоравањем протока на врху, што деградира конвективни пренос топлоте и фаворизује кондуктивни, посебно при високим  $Gr$ .

Остали тестирани случајеви показују да случај са две елипсе нуди најбољу термичку хомогеност и значајно смањује проблем успоравања протока. Овај

резултат је предложен као решење за проблем термичке стратификације.